Spectrochimica Acta Part A: Molecular and Biomolecular Spectroscopy 143 (2015) 59–66

Contents lists available at ScienceDirect

Spectrochimica Acta Part A: Molecular and Biomolecular Spectroscopy

journal homepage: www.elsevier.com/locate/saa

Intra- and intermolecular hydrogen bonding and conformation in 1-acyl thioureas: An experimental and theoretical approach on 1-(2-chlorobenzoyl)thiourea

Aamer Saeed [a,*], Asma Khurshid [a], Michael Bolte [b], Adolfo C. Fantoni [c], Mauricio F. Erben [d,*]

[a] Department of Chemistry, Quaid-I-Azam University, Islamabad 45320, Pakistan
[b] Institut für Anorganische Chemie, J.W.-Goethe-Universität, Max-von-Laue-Str. 7, D-60438 Frankfurt/Main, Germany
[c] Instituto de Física La Plata, Departamento de Física, Facultad de Ciencias Exactas, Universidad Nacional de La Plata, 49 y 115, La Plata, Buenos Aires, Argentina
[d] CEQUINOR (UNLP, CONICET-CCT La Plata), Departamento de Química, Facultad de Ciencias Exactas, Universidad Nacional de La Plata, C.C. 962 (1900), La Plata, Buenos Aires, Argentina

HIGHLIGHTS

- Crystal structures and vibrational properties were determined.
- The C=O and C=S double bonds of the acyl-thiourea group are mutually oriented in opposite directions.
- The $-NH_2$ is involved in strong N–H···O=C intramolecular hydrogen bond.
- Both, thioamide (N–H) and carbamide ($-NH_2$) groups participate in intermolecular N–H···S=C hydrogen bonds.
- Topological analysis reveals a Cl···N interaction playing a relevant role in crystal packing.

GRAPHICAL ABSTRACT

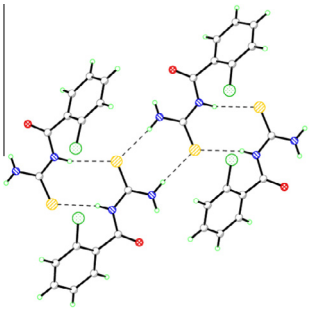

ARTICLE INFO

Article history:
Received 10 October 2014
Received in revised form 2 February 2015
Accepted 9 February 2015
Available online 14 February 2015

Keywords:
Thiourea
Crystal structure
Vibrational spectroscopy
Hydrogen bond
NBO
AIM topological analysis

ABSTRACT

The vibrational analysis (FT-IR and FT-Raman) for the new 1-(2-chlorobenzoyl)thiourea species suggests that strong intramolecular interactions affect the conformational properties. The X-ray structure determination corroborates that an intramolecular N–H···O=C hydrogen bond occurs between the carbonyl (–C=O) and thioamide ($-NH_2$) groups. Moreover, periodic system electron density and topological analysis have been applied to characterize the intermolecular interactions in the crystal. Extended N–H···S=C hydrogen-bonding networks between both the thioamide (N–H) and carbamide (NH_2) groups and the thiocarbonyl bond (C=S) determine the crystal packing. The Natural Bond Orbital (NBO) population analysis demonstrates that strong hyperconjugative remote interactions are responsible for both, intra and intermolecular interactions. The Atom in Molecule (AIM) results also show that the N–H···Cl intramolecular hydrogen bond between the 2-Cl-phenyl ring and the amide group characterized in the free molecule changes to an N···Cl interaction as a consequence of crystal packing.

Introduction

Very recently, Eccles at al. [1] demonstrate the versatility of the thioamide functional group [–C(S)NH_2] as a key moiety for crystal

* Corresponding authors. Tel.: +92 51 9064 2128; fax: +92 51 9064 2241 (A. Saeed). Tel./fax: +54 221 425 9485 (M.F. Erben).
E-mail addresses: aamersaeed@yahoo.com (A. Saeed), erben@quimica.unlp.edu.ar (M.F. Erben).

http://dx.doi.org/10.1016/j.saa.2015.02.042
1386-1425/

engineering. The related acetylthiourea species, CH_3-C(O)NHC(S)NH_2, has been known for more than a century [2] and represents the first example of the 1-acyl-thiourea family of compounds [–C(O)NHC(S)NH_2] [3–5]. Its X-ray structure was early reported [6], resulting in an molecular structure in which the heavy atoms skeleton are arranged in a planar fashion with the carbonyl double bond interacting *via* an intramolecular hydrogen bond with the –NH_2 group. The infrared and Raman spectra were also interpreted in terms of a C_S point group model [7]. More recent quantum chemical calculations on small model compounds [8] reveal that the central –C(O)NHC(S)NH_2 group can display several conformations, depending on the dihedral values around the acyl-N bond and the adjacent N–C bond [9].

For 1-(acyl/aroyl)-3-(mono-substituted) thiourea derivatives a local planar structure of the thiourea moiety is preferred, with opposite orientation between the C=O and C=S double bonds (''*S*-shape'') [10]. In this conformation, a pseudo six-membered ring structure promotes a C=O···H–N intramolecular hydrogen bond. On the other hand, when the formation of a suitable hydrogen bond is prevented, as in 1-(acyl/aroyl)-3,3-(di-substituted) thiourea derivatives (R^2, $R^3 \neq$ H), the *anticlinal* geometry (*U* form) is preferred [11–14].

The understanding of the conformational properties on these compounds has direct relevance in applied fields, including chemosensors for selective and sensitive naked-eye recognition for anions [15–18] and new developments on biological [19] and pharmaceutical applications [20–22]. As has been recognized, the success of many of these applications of 1-acyl thioureas, rely on the formation of proper hydrogen bonds with particular receptors [23]. The 2-chlorophenylthiourea compound effectively coordinate zinc (II) cations in the presence of acetylacetonate forming a screw shaped square-pyramidal coordination compound with promising application in nonlinear optics [24].

Continuing our project dedicated to the study of 1-(acyl/aroyl)-3-(mono-substituted) thioureas [25,26], in this article the preparation of the new species 1-(2-chlorobenzoyl)thiourea is presented. It is interesting to note that although several thioureas containing the 1-(2-chlorobenzoyl) group with different degree of substitution at the second nitrogen atom have been reported [27–31], the non-substituted species remains unknown. In this work, the molecular and crystal structures in conjunction with the vibrational properties have been determined by X-ray diffraction and spectroscopic (infrared and Raman) analysis of the solid. These studied have been complemented by quantum chemical calculations. In particular the Natural Bond Orbital (NBO) [32,33] population analysis has been performed in order to evaluate the donor → acceptor intra and intermolecular interactions for the monomer and also for dimer and trimer arrangements of molecules. Finally, to better characterize the intermolecular interactions present in the crystal and the possible effect of packing in the intramolecular interactions, the topology of the electron density obtained from a periodic quantum calculation has been analyzed by using the atoms in molecules (AIM) approach [34].

Experimental

Synthesis and characterization

Following the method reported for related species [35], freshly prepared 2-chlorobenzoyl chloride was added to a solution of potassium thiocyanate in acetone to get the corresponding isothiocyanate *via* stirring at room temperature for 1 h. The *in situ* formed 2-chlorobenzoyl isothiocyanate was treated with aqueous ammonia at low temperature. On completion of the reaction mixture was poured in ice cold water and the solid product obtained was recrystallized from ethanol to afford yellow crystalline solid.

Yield: 85%; m.p: 152 °C; IR (cm^{-1}): 3329, 3153, 1687, 1236; ^{1}H-NMR (ppm, $CDCl_3$, 300 MHz): 11.64 (s, CON**H**, 1H), 9.64 (CSN$\mathbf{H_2}$, 2H), 7.52 (m, 3H, Ar), 7.41(m, 1H Ar); ^{13}C-NMR ($CDCl_3$, 75 MHz): 182.0 (**C** = S), 167.7 (-**C**O), 135.0, 132.3, 130.31, 130.0; GC–MS: 139 (M^+), 111, 85, 75, 44; elemental analysis: Calcd. For $C_8H_7ClN_2OS$ C: 44.76, H: 3.29, N: 13.05, S: 14.94%. Found C: 44.70, H: 3.11, N: 13.02, S: 14.90%.

Instrumentation

Melting point was determined using a digital Gallenkamp (SANYO) model MPDBM3.5 apparatus and was uncorrected. ^{1}HNMR and ^{13}C NMR spectra were determined in $CDCl_3$with a 300 MHz Bruker AM-300 spectrophotometer. Mass Spectra (EI, 70 eV) were taken on a GC–MS, Agilent technologies 6890N with an inert mass selective detector 5973 mass spectrometer and elemental analyses were conducted using a LECO-183 CHNS analyzer.

Vibrational spectroscopy

Solid-phase (in KBr pellets) infrared spectra were recorded with a resolution of 2 cm^{-1} in the 4000–400 cm^{-1} range on a Bruker EQUINOX 55 FTIR spectrometer. FTIR spectra (ATR) were recorded on an a Bio-Rad-Excalibur Series Mode FTS 3000 MX spectrophotometer. The FT-Raman spectra of the powdered solid sample were recorded in the region 4000–100 cm^{-1} using a Bruker IFS 66v spectrometer equipped with Nd:YAG laser source operating at 1.064 μm line with 200 mW power of spectral width 2 cm^{-1}.

Computational details

Molecular quantum chemical calculations have been performed with the GAUSSIAN 03 program package [36] by using the B3LYP DFT hybrid methods employing Pople-type basis set [37]. The moderate 6-31G(d,p) basis set has been applied for the relaxed scan calculations, whereas the extended valence triple-ξ basis set augmented with diffuse and polarization functions in both the hydrogen and weighty atoms [6-311++G(d,p)] has been used for geometry optimization and frequency calculations. The calculated vibrational properties corresponded in all cases to potential energy minima for which no imaginary frequency was found. The recommended scale factor of 0.96 has been applied for analyzing the theoretical harmonic vibrational frequencies [38]. Periodic calculations were performed at the B3LYP/6-31G(d,p) level with Crystal98 and Crystal09 codes [39,40]. Using the experimental estimations as the starting point, the coordinates of the hydrogen atoms in the crystal were optimized to minimize the B3LYP/6-31G(d,p) crystal energy with heavy atom coordinates and cell parameters fixed at their experimental values. The topology of the resulting electron density was then analyzed using the TOPOND98 program [41]. For consistency with the periodic results, molecular and supramolecular electron densities were also analyzed with TOPOND98 from calculations performed with Crystal98 using geometry optimized with Crystal09.

X-ray data collection and structure refinement

X-ray data were collected on a STOE IPDS-II diffractometer with graphite-monochromated MoKα radiation. An empirical absorption correction with the PLATON program [42] was performed. The structure was solved by direct methods and refined with full-matrix least-squares on *F*2 using the program SHELXL97 [43]. H-atoms bonded to carbon atoms were placed on ideal positions and refined with fixed isotropic displacement parameters using a riding model. H-atoms bonded to N were freely refined. Full crystallographic data have been deposited with the Cambridge Crystal-

lographic Data Centre (CCDC). Enquiries for data can be directed to: Cambridge Crystallographic Data Centre, 12 Union Road, Cambridge, UK, CB2 1EZ or (e-mail) deposit@ccdc.cam.ac.uk or (fax) +44 (0) 1223 336033. Any request to the Cambridge Crystallographic Data Centre for this material should quote the full literature citation and the reference number CCDC 988811.

Results and discussion

Synthesis and characterization

The title compound was prepared by reaction of 2-chlorobenzoylisothiocyanate with aqueous ammonia at low temperature. The isothiocyanate was obtained *in situ* by stirring 2-chlorobenzoyl chloride with potassium thiocyanate in dry acetone at room temperature for one hour. The product was re-crystallized from ethanol as yellow crystals in high yield. The ^{1}H NMR spectrum showed singlets of one and two protons at δ 11.64 and 9.64 ppm for CONH, and $CONH_2$ respectively besides the multiplets at 7.52–7.41 for aromatic protons. In ^{13}C NMR the characteristic thiocarbonyl and carbonyl carbons appeared at 182.0 and 167.7 ppm, respectively, in addition to other characteristic signals.

Tautomerism and molecular conformation

Thione-thiol tautomerism is plausible for 1-acyl thioureas, the thione form being strongly preferred [44], although the presence of minor amount of the thiol form in the solid phase has been suggested [45,46]. This tautomeric equilibrium is similar to that found for thiobiuret analogs, for which the interplay of conjugative stabilization and intramolecular hydrogen bonding defines the tautomeric preferences [47]. The two main tautomeric forms expected for the title compound have been computed at the B3LYP/6-311++G(d,p) level of approximation and the optimized structure are shown in Fig. 1. According to these calculations, the *S*-thione form is more stable than the thiol form by 18.2 kcal/mol ($\Delta E°$ values, including zero point energy) for the molecule isolated in a vacuum.

To further inspect the potential energy surface of the thione tautomer, the potential energy function for internal rotation around the central N–C dihedral angle has been calculated. The B3LYP/6-31G(d,p) level of approximation has been applied allowing geometry optimizations with the corresponding dihedral angle varying from 0° to 180° in steps of 10°. The potential energy curve is shown in Fig. 2.

A clear minimum at δ(C7N1–C8N2) = 0° is observed, corresponding to a local planar structure of the central –C═O–NH–C═S– moiety, with opposite orientation between the C═O and C═S double bonds. This conformation corresponds to the *S* form showed in Fig. 1. Moreover, the structures with δ(C7N1–C8N2) = 180° correspond to a local maxima in the potential energy curve. Two nearly equivalent local minima are observed at δ(C7N1–C8N2) values of ca. 150° and 210°, corresponding to non-planar synclinal

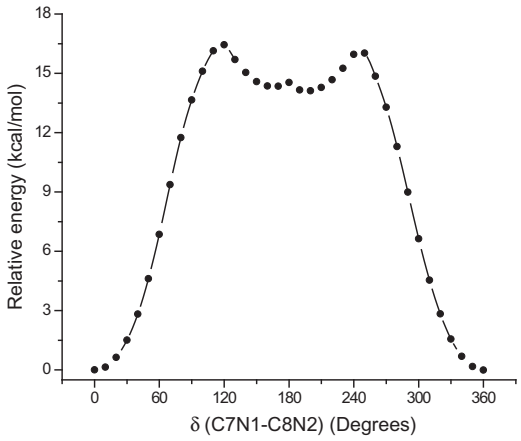

Fig. 2. Calculated [B3LYP/6-31G(d,p)] potential function for internal rotation around the δ(C7N1C8N2) dihedral angle of 1-(2-chlorobenzoyl)thiourea. For atom numbering see Fig. 1.

conformers ("*U*" form, see Fig. 1) and are located higher in energy by ca. 13.2 kcal mol^{-1}. These results are in good agreement with the structural analysis based on 739 structures containing the –C(C═O)N(C═S)N– moiety deposited in the Cambridge Structural Database [10]. The prevalence for the *S* conformation is clearly established for 1-(acyl/aroyl)-3-(mono-substituted) thiourea derivatives, showing a local planar structure of the central –C(O)–NH–C(S)–NH– moiety, with opposite orientation between the C═O and C═S double bonds. In this conformation the C═O and H–N groups form a pseudo 6-membered ring, favoring an intramolecular interaction through a hydrogen bond [11,28,48].

The potential energy curve for the rotation of the 2-chlorophenyl ring with respect to the thiourea group is shown in Fig. 3. As expected, the curve is symmetric with respect to the planar thiourea group, with two minima at dihedral angles of ca. 40° and 130°, the former being more stable by ca. 1 kcal/mol. The occurrence of planar arrangements between the 2-chlorophenyl and the amide-like groups are disfavored, the structures with N1C7–C1C2 torsion angle having values of 0° and 180° being clear maxima in the potential energy curve.

Vibrational analysis

The FT-IR, attenuated total reflectance (ATR-FTIR) and FT-Raman spectra for the title compound in the solid phase were measured as KBr pellets and pure powdered samples, respectively. Very similar FTIR spectra were obtained for the transmittance and ATR modes, the first one giving slightly better band separations especially in the 1000–400 cm^{-1} spectral region. The observed wavenumbers and those calculated at the B3LYP/6-311++G(d,p) level for the *S* form of the isolated molecule are reported in Table 1, together with a tentative assignment of the bands. The assignment has been carried out by comparison with theoretical wavenumbers as well as on comparison with the reported data for $CH_3C(O)NHC(S)NH_2$

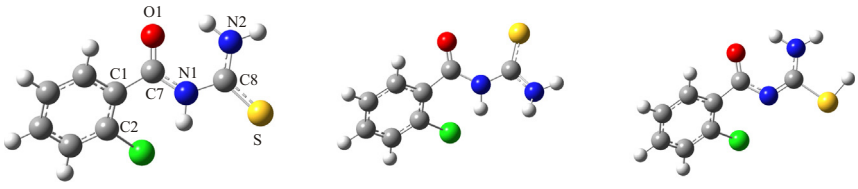

Fig. 1. Molecular structures optimized [B3LYP/6-311++G(d,p)] for the thione (in the *S* and *U* conformations) and thiol tautormers of 1-(2-chlorobenzoyl)thiourea. Relative energies values ($\Delta E°$, in kcal/mol) are given.

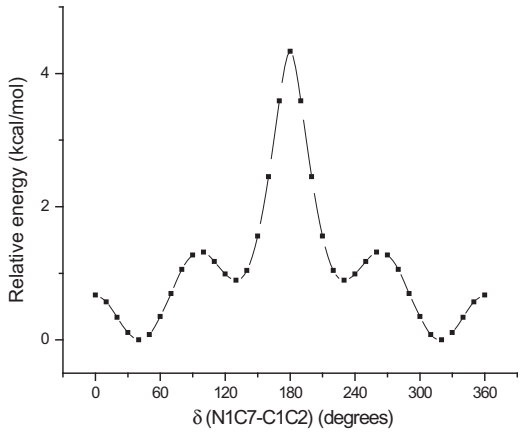

Fig. 3. Calculated [B3LYP/6-31G(d,p)] potential function for internal rotation around the C1–C7 bond, i.e. for the rotation of the 2-Cl-phenyl group with respect to the amide group of 1-(2-chlorobenzoyl)thiourea. For atom numbering see Fig. 1.

[7,49] and related thioureas containing the chlorobenzoyl group [30,50–52]. Special attention was dedicated to the band assignment of the normal modes associated with the central acyl thiourea group.

A series of absorptions appearing in the high energy region (3500–2500 cm^{-1}) of the infrared spectrum are associated with the N–H and C–H stretching modes. With the help of quantum chemical calculations, the absorptions appearing at 3324 and 3114 cm^{-1} can be assigned to the antisymmetric and symmetric N–H stretching vibration of the $–NH_2$ group, respectively. The low value corresponding to the symmetric motion is probably due to the fact that this mode is mostly influenced by the intramolecular C═O···H–N1 hydrogen bond [53]. The separation between $\nu_{as}(NH_2)$ and $\nu_s(NH_2)$ is well reproduced by the B3LYP/6-311++G(d,p) calculations (203 cm^{-1}) given confidence to this tentative assignment. A third band located at intermediate values (3246 cm^{-1}) is assigned to the N–H stretching of the thioamide group [52].

The intense absorption at 1684 cm^{-1} corresponds to the ν(C═O) stretching mode [54,55], in agreement with that found for the parent $CH_3C(O)NHC(S)NH_2$ species occurring at 1680 cm^{-1} [7]. The computed [B3LYP/6-311++G(d,p)] infrared spectra for the *S* form predicts this mode as an intense absorption at 1649 cm^{-1}, whereas for the *U* conformer it is computed at 1779 cm^{-1}, in a clear indication that the N1–H···O═C intramolecular interaction is responsible for the red-shift and high intensity of the ν(C═O) mode observed for the *S* form [12,54,56]. This description is well complemented by the analysis of the Raman spectrum, where a strong signal appears at 1682 cm^{-1}. It is plausible that the intensity observed for ν(C═O) in the Raman spectrum is increased by the formation of inter and intramolecular hydrogen bonds [57,58].

The infrared spectrum shows two very strong absorptions at 1619 and 1547 cm^{-1}, which are tentatively assigned to the δ(N–H) deformation modes on the $–NH_2$ group and N1–H acyl thiourea group, respectively [56]. Quantum chemical calculations for the *S* form confirm the presence of very intense absorptions at 1549 and 1480 cm^{-1} (scaled values), whose displacement vectors allow the assignment of these fundamentals to the δ(N–H) deformation modes. Agreement is also found when the spectra is compared with those reported for $CH_3C(O)NHC(S)NH_2$ and its tri-deuterated analogue [7]. In effect, the δ(N–H) deformation modes on the $–NH_2$ and –NH– groups contribute to strong absorptions at 1590 and 1525 cm^{-1}, respectively.

The ν(C═S) stretching is tentatively assigned to the medium intensity absorption observed at 801 cm^{-1}, with an strong counterpart in the Raman spectrum at 798 cm^{-1}, in good agreement with the computed value of 780 cm^{-1} [B3LYP/6-311++G(d,p)] and with reported data for related species [12,45]. In particular, for $CH_3C(O)NHC(S)NH_2$ this mode contributes mainly to the absorption appearing at 820 cm^{-1} in the infrared spectrum [7].

Table 1
Experimental FTIR (in transmittance and attenuated total reflectance modes) and Raman, as well as theoretical [B3LYP/6-311++G(d,p)] vibrational data (cm^{-1}) with a tentative assignment for 1-(2-chlorobenzoyl)thiourea.

Experimental[a]			Computed[b]	Tentative assignment[c]
FTIR	ATR-FTIR	Raman		
3324 s	3329 s		3545(120)	$\nu_{as}(NH_2)$
3246 m	3232 m		3453(48)	ν(N-H)
3114 m, br	3120 m	3122 vw	3350(150)	$\nu_s(NH_2)$
3058 sh	3023 w	3063 s	3075(1)	ν(C–H)′s ring
2988 m			3063(6)	
2916 m		3024 vw	3051(2)	
2788 m			2906(5)	
1684 s	1687 s	1682 s	1649(206)	ν(C═O)
			1566(22)	ν(C═C)
1619 vs	1603 vs	1619 w	1549(390)	$\delta(NH_2)$
1598 sh	1598 sh	1592 s	1537(21)	ν(C═C)
		1570 m,sh		
1547 vs	1538 vs	1547 w	1480(747)	δ(N–H)
1471 m	1471 m		1437(18)	ν(C═C)
1436 m	1434 m	1437 w	1404(25)	ν(C═C)
1403 s	1402 br	1404 w	1340(270)	ν_{as}(NCN)
1342 w		1350 vw	1280(32)	ν_s(NCN)
1315 w		1312 vw	1265(7)	ν(C═C)
1289 vs			1235(85)	δ(C–H)
1275 sh	1279 s	1288 s	1195(190)	ν((O)C–C)
1265 vs	1270 sh	1262 sh	1140(2)	δ(C–H)
1254 vs	1237 vs	1251 s	1101(111)	ν(C═C)
1165 m	1162 m	1166 s	1098(70)	ν(C–N(H))
1135 s	1122 vs	1132 m	1022(170)	δ(C–H)
1126 sh	1117 sh			
1055 s	1049 s	1054 sh	1011(93)	δ(CCC)
1049 sh	1038 s	1039 vvs		
1019 vs	1010 vs	1017 m	967(151)	ρNH_2
1005 vs		988 m	965(114)	ρ(C–H)
986 vs				
976 sh			937(3)	ρ(C–H)
947 m	953 m	948 vw	887(42)	δ(CNC)
913 w	909 w	912 vs	851(2)	ρ(C–H)
870 m	875 m	869 w		
830 w		828 m		
801 m	796 m	798 s	780(31)	ν(C═S)
771 m	766 m	779 w	766(10)	ρ(C–H)
764 m		764 m	731(52)	ρ(C–H)
744 s	745 s,br		705(20)	δ(C–C)
725 w		724 w	681(10)	ν(C–Cl)
703 m		704 vw	649(4)	$\rho(NH_2)$
695 sh	695 m	694 vw	628(13)	δ(CCC)
662 sh,m		641 s		
644 m	641 s	634 sh	615(33)	ρ(NH)
627 m	603 s,br	622 vs	592(42)	oop(C═S)
563 w		565 w	528(1)	δ(CCN)
478 m		477 s	468(13)	δ(CCC)
469 vvw			450(4)	δ(NCS)
460 m	462 m		436(159)	$\rho(NH_2)$
432 vw	425 w	432 s	418(6)	δ(NCN)
416 w			412(4)	δ(CCC)
		370 m	350(1)	δ(NCS)
		358 m,br	322(17)	δ(CCCl)
		347 sh		
		314 m	249(1)	δ(CCC(O))
		269 m		
		251 m	234(11)	ρ(C(O))
		223 m	209(2)	ρ(NCN)
		190 m	146(1)	ρ(NCS)
		167 m	103(2)	τ

[a] FTIR of solid in KBr pellets, ATR-FTIR and FT-Raman of finely powdered solid. Band intensity: vs = very strong, s = strong, m = medium, w = weak, vw = very weak, vvw = very very weak, sh = shoulder band.

[b] Scaled computed values for the *S* form. In parentheses relative band strengths, IR intensities [in km/mol].

[c] ν: stretching (subscripts s and as refer to symmetric and antisymmetric modes, respectively), δ: deformation, ρ: rocking, oop: out of plane deformation and τ torsional modes.

Molecular and crystal structure

1-(2-chlorobenzoyl)thiourea crystallizes in the triclinic space group *P*-1 (see Table 2), with two molecules in the asymmetric unit, as shown in Fig. 4. Both molecules are in the *S*-conformation. A least-square fit of all non-H atoms (r.m.s. deviation 0.115 Å) shows that there are no remarkable differences between the two molecules, as can be observed in Fig. 5.

The carbonyl oxygen in the amide group is slightly out of the mean plane of the benzene ring, the N1–C7–C1–C2 torsion angle being 50.8(2)°, in reasonable agreement with the computed value for the free molecule of 40.9° (see Fig. 3). Similar conformational features were reported for chloro-benzoyl thioureas [59,60]. Bond lengths and angles in the heavy atom skeletons are within normal ranges [61,62] (see Tables S5 and S6 in the Supplementary data).

A schematic view along *c*-axis (see Fig. 6) makes evident that 1-(2-chlorobenzoyl)thiourea crystal can be considered as having a layered structure. At this respect it is interesting to note that S atoms as well as N–H and NH_2 groups are all very near to the mean planes defined by themselves, parallel to (*a*,*b*) and facing each others. But also Cl atoms are all very near to planes parallel to (*a*,*b*) nearly midway along *c*-axis between those previously mentioned. As we will see in what follows, those geometrical features would be closely related to the way molecules interconnect.

Table 2
Crystal data and structure refinement for 1-(2-chlorobenzoyl)thiourea.

Empirical formula	$C_8H_7ClN_2OS$
Formula weight	214.67
Temperature	173(2) K
Wavelength	0.71073 Å
Crystal system	Triclinic
Space group	*P*-1
Unit cell dimensions	a = 8.3240(7) Å, α = 66.197(7)°
	b = 10.5091(10) Å, β = 88.842(7)°
	c = 12.3602(11) Å, γ = 69.805(7)°
Volume	919.48(14) $Å^3$
Z	4
Density (calculated)	1.551 Mg/m^3
Absorption coefficient	0.600 mm^{-1}
F(000)	440
Crystal size	0.48 × 0.47 × 0.47 mm^3
Theta range for data collection	3.63–25.57°
Index ranges	−10 <= h <= 9, −12 <= *k* <= 12,
	−14 <= l <= 14
Reflections collected	7819
Independent reflections	3416 [*R*(int) = 0.0267]
Completeness to theta = 25.00°	99.4%
Absorption correction	Semi-empirical from equivalents
Max. and min. transmission	0.7659 and 0.7618
Refinement method	Full-matrix least-squares on F^2
Data/restraints/parameters	3416/0/260
Goodness-of-fit on F^2	1.064
Final *R* indices [*I* > 2sigma(I)]	R1 = 0.0274, wR2 = 0.0715
R indices (all data)	R1 = 0.0297, wR2 = 0.0730
Extinction coefficient	0.020(2)
Largest diff. peak and hole	0.280 and −0.199 e.$Å^{-3}$

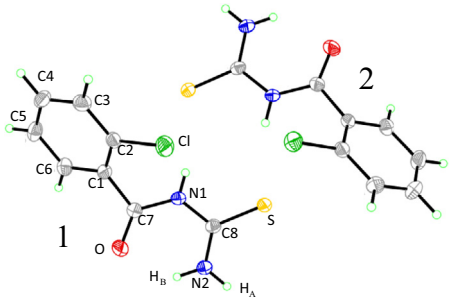

Fig. 4. Asymmetric unit of the title compound in a single crystal at 173 K. Labels 1 and 2 stand for each molecule within the asymmetric unit (anisotropic displacement ellipsoids drawn at the 50% probability level).

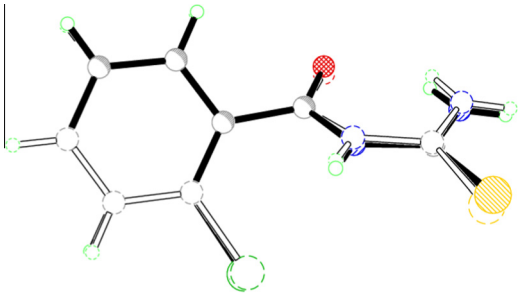

Fig. 5. Superposition of the two molecules of the asymmetric unit.

Topology analysis of the electron densities

Since many of the more relevant intra and intermolecular interactions involve hydrogen atoms, their positions in the crystal were optimized at the B3LYP/6-31G(d,p) level, keeping fixed at their crystallographic values the heavy atom positions and cell parameters. The electron density topology of this partially optimized crystal structure was then analyzed. Values of the electron density and positive principal curvature of the Laplacian at the corresponding (3,−1) critical point were used as indicators of the interaction strength [63].

Topological parameters of the predominant intermolecular interactions are reported in Table 3. The main two are N–H···S=C interactions connecting each other molecules 1 and 2 of the asymmetric unit (see Fig. 7a). Both of them have very similar topological characteristics and form a cyclic motif. The only other two interactions with strengths similar to those previously mentioned connect molecule 1 of a reference asymmetric unit with molecule 2 generated by [−1 + *x*, *y*, *z*], linking the sulfur atom of one molecule to an amino hydrogen atom of the other one, forming a cyclic motif, as is also shown in Fig. 7a. Following Berstein et al. [64], both yet described motifs can be classified as $R_2^2(8)$ since they form pseudo eight-membered rings with two donors and two acceptors each. On geometrical grounds, the four N–H···S=C interactions involved can be considered hydrogen bonds. Alternation of both kinds of cyclic motifs gives rise to infinite chains along *a* axis. Similar patterns are commonly encountered in 1-acyl-thioureas [14],[65,66]. Only the sulfur atom of molecule 1 is in addition interacting with two aromatic hydrogen atoms, one belonging to the molecule 1 generated by [1 − *x*, 1 − *y*, −*z*] and the other to the molecule 2 generated by [1 − *x*, 1 − *y*, 1 − *z*], as shown in Fig. 7b. With all probability the slight difference in molecular geometry between molecules in the asymmetric unit is mainly a consequence of such a difference in intermolecular interactions. Another medium weak interaction links chlorine atom of molecule 1 with an aromatic hydrogen atom of molecule 2 generated by [1 − *x*, −*y*, 1 − *z*] (see Fig. 7b).

Backing to the layer-like structure described in the previous section, it is worth noticing that bond paths of the strongest interactions are all around the mean planes parallel to (***a***,***c***) defined by the N1–H and –NH_2 groups and S atoms and that could be considered the layer boundaries. Layers are linked one each other through C–H_{ar}···S interactions, while molecules within a layer are connected through C–H_{ar}···Cl interactions and the weakest C–H_{ar}···S ones.

Differences in geometry and electron density topology between the in-crystal and free molecules deserve some comments. Rele-

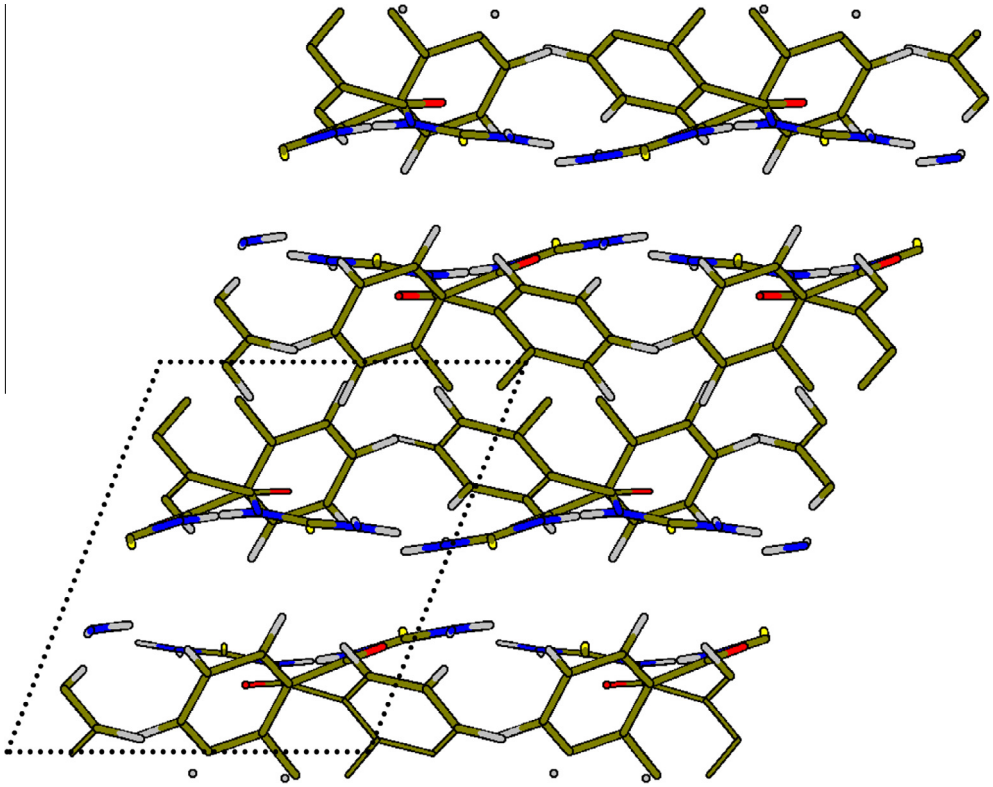

Fig. 6. View along ***c***-axis of the 1-(2-chlorobenzoyl)thiourea crystal packing.

Table 3
Topological properties (a.u.) and geometrical parameters (Å and °) of the intramolecular and main intermolecular interactions in the B3LYP/6-31G(d,p) electron density of the 1-(2-chlorobenzoyl)thiourea crystal and molecule: electron density (ρ), laplacian ($\nabla^2\rho$) and positive principal curvature (λ_3) evaluated at the corresponding (3,−1) critical points.

Attractors[a,b]		ρ	$\nabla^2\rho$	λ_3	H···A	D–H···A
Intermolecular						
S(1)	HN1(2)	0.0210	0.0450	0.0894	2.372	159.3
S(2)	HN1(1)	0.0212	0.0448	0.0896	2.368	161.4
S(1)	$H_AN2(2^I)$	0.0188	0.0437	0.0828	2.412	160.5
$S(2^I)$	$H_AN2(1)$	0.0184	0.0416	0.0800	2.417	175.7
S(1)	$H_{ar}C6(1^{II})$	0.0097	0.0293	0.0446	2.797	141.3
S(1)	$H_{ar}C6(2^{III})$	0.0079	0.0253	0.0378	2.820	160.1
Cl(1)	$H_{ar}C4(2^{IV})$	0.0083	0.0278	0.0422	2.766	152.1
Intramolecuar[c]						
O	H_BN2	0.0289	0.0909	0.1639	1.953	127.3
		0.0327	0.1026	0.1896	1.888	130.7
Cl	N1	0.0120	0.0451	0.0580	2.760	72.7[d]
	HN1	0.0152	0.0589	0.0856	2.470	119.7

[a] Between parenthesis the label identifying molecule, including symmetry code as a superscript. In the second column attractor is the hydrogen atom.
[b] Symmetry codes: I: $-1+x, y, z$; II: $1-x, -y, -z$; III: $1-x, 1-y, 1-z$; IV: $1-x, -y, 1-z$.
[c] First row: in-crystal molecule; second row: free molecule.
[d] Though attractor is N1 the value of N1–H···Cl is reported.

vant geometric and topological parameters are reported in Table 3. Data obtained from a geometry optimization at the B3LYP/6-31G(d,p) level are used for the free molecule. Packing induces significant changes in some bond lengths and angles but, most important, in the geometry of the non-bonded intramolecular contacts. From a topological view point the most significant change on going from the free molecule to the in-crystal one is the switch from an N–H···Cl hydrogen bond to an H–N···Cl interaction. On geometrical grounds this behavior is consistent with the rather significant enlargement of the Cl···H distance and decrease of the Cl···H–N angle, whose value in the crystal is far outside the accepted range for hydrogen bond interactions [67].

In order to get more hints on this behavior we decided to perform a supramolecular geometry optimization on the isolated asymmetric unit molecular pair. Though changes in the pair geometry with respect to the in-crystal one are observed, molecular geometry is closer to that within the crystal than to the free molecule one. More importantly, from a topological view point intramolecular interactions in the pair resemble those in the crystal. Although contributions from other intermolecular interactions are expected, the rather drastic changes in molecular geometry and electron density topology on going from the free to the in-crystal molecule can then mainly be attributed to interactions within the asymmetric unit.

Natural Bond Orbital analysis

It has been suggested that electronic donor–acceptor interactions between remote orbitals deserve close inspections owing to the influence they can play on the backbone conformation [68]. In the frame of the Natural Bond Orbital (NBO) population analysis the energy of these donor–acceptor interactions can be estimated by the second order perturbation theory [69].

Recently, we have demonstrated that a remote lpO → σ^*(N–H) interaction takes place for the *S* form in acyl-thiourea species [70], amounting to as much as 12.03 kcal/mol, a value that is higher than that found for benzenesulfonylamin acetamide molecules (9.5 kcal/mol) [71]. This remote lpO → σ^*(N2–H) hyperconjugative interaction can be also confirmed as acting in the title species. In effect, the second order perturbation analysis performed at the B3LYP/6-311++G(d,p) level of approximation, computes a donor–acceptor stabilization energy of 8.2 kcal/mol, which is responsible for the electrostatic character present in "classical" C═O···H–N2 hydrogen bond [72]. It is worth noting that this remote interaction

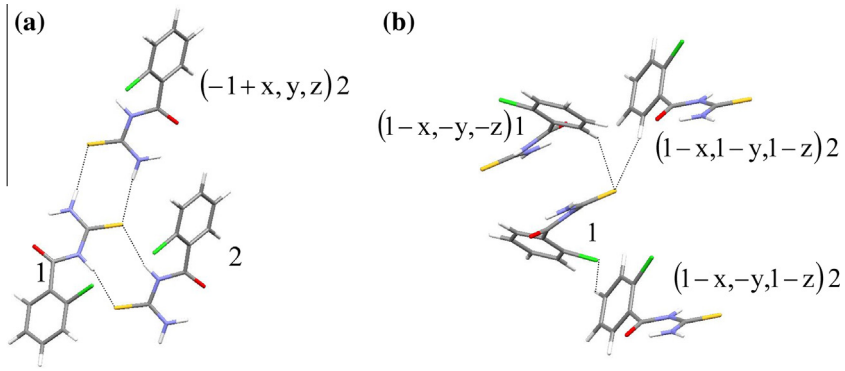

Fig. 7. Main intermolecular interactions in the crystal of 1-(2-chlorobenzoyl)thiourea. (a) N-H···S=C building $R_2^2(8)$ motifs. (b) C–H_{ar}···S and C–H_{ar}···Cl. Between parenthesis the symmetry operation generating the molecule.

occurs through the pseudo-six member ring and; due to the orientation request for the orbital overlapping, it is feasible only for the *S* conformation.

Interestingly, in agreement with the topological analysis, a remote interaction of the type lpCl → σ^*(N1–H) is observed, involving the pseudo-six member formed between the C–Cl and the H–N1 group in the 2-chlorobenzyl amide moiety. This partial transfer of a lone pair of electrons of chlorine atom to the N1–H antibonding orbital corresponds to a weak (1.4 kcal/mol) but undoubtedly important interaction.

In order to scrutinize the donor → acceptor interactions between molecules, the NBO analyses have also been applied for a dimer and trimer arrangement of molecules as observed in the crystal structure. Thus, starting from the positions found in the X-ray analysis, optimization of the geometry and NBO analysis at the B3LYP/6-311++G(d,p) level of approximation have been performed. The optimized structures are shown in Figs. S1 and S2 given as Supporting material.

For the centro-symmetric dimer, the computed C=S bond length (1.681 Å) is longer than that computed for the monomer (1.669 Å), whereas the N1–C8 bond length is longer in the monomer than that of the dimer, with values of 1.403 and 1.390 Å, respectively. Similar trends are observed in the trimer arrangement, with the C=S bond distance of molecule 1 elongated up to 1.696 Å with an N1–C8 bond length of 1.390 Å. The computed hydrogen bond is characterized by a S···H–N1 distance of 2.46 Å and S···H–N1 angle of 161.3° in the dimer. When the trimer is analyzed, similar values are observed between molecules 1 and 2, with S···H(N1) distance and S···H–N1 angle of 2.45 Å and 165.6°. The second C=S···H–N2 interaction – with the molecule located at (−1 + *x*, *y*, *z*) occurring through the –C(S)NH_2 group, see Fig. 7a is characterized by S···H(N2) distance and S···H–N2 angle of 2.44 Å and 170.4°, respectively. The experimental mean values are 2.56(2) and 2.55(2) Å for the S···H–N distances and 161(2)° and 167.2° for the bond angles of the C=S···H–N interactions involving the N1 and N2 nitrogen atoms, respectively (see Table 3 for comparison).

The second order perturbation analysis clearly identified the electron donation from the sulfur lone pair orbitals of one molecule toward the σ^*(N1–H) antibonding orbital formally localized on the amide-like group of the second molecule in the dimer. The remote lpS → σ^*(N1–H) interaction between the two units in the dimer amounts as much as 12.9 kcal/mol. This electron donation is also observed in the trimer arrangement with a similar strength (13.1 kcal/mol).

The C=S···H–N2 interaction involving the –NH_2 terminal group was analyzed by studying the donor–acceptor electron donation between molecule 1 and the second molecule located at the

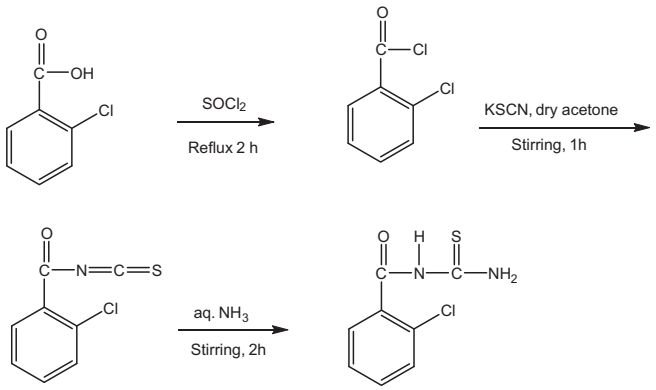

Scheme 1. Synthesis of 1-(2-chlorobenzoyl)thiourea.

(−1 + *x*, *y*, *z*) position (see Fig. 7a). In this case, the remote lpS → σ^*(N2–H) interaction amounts to 12.5 kcal/mol [σ^*(N2–H) antibonding orbital formally localized on the –NH_2 group] (see Scheme 1).

Thus, the NBO analysis allows interpreting the intramolecular C=S···H–N hydrogen bonds involving the thiourea group as (remote) donor → acceptor electron transfer between the lone pair electrons of the sulfur and the σ^*(N–H) antibonding orbitals of both the N1–H and –NH_2 groups. Moreover, the computed lpS → σ^*(N–H) values are similar, suggesting similar strength for both C=S···H–N intermolecular hydrogen bonds.

Conclusions

The molecular and crystal structures of the novel species 1-(2-chlorobenzoyl)thiourea are strongly determined by intramolecular and intermolecular hydrogen bond. The formation of an intramolecular C=O···H–N2 hydrogen bond is promoted by an lpO → σ^*(N2–H) hyperconjugative interaction that favors the adoption of the *S* conformation of the 1-acyl thiourea group. Low frequency values observed in the vibrational spectra (infrared and Raman) for the ν(C=O) (1684 cm^{-1}) and $\nu_s(NH_2)$ (3114 cm^{-1}) stretching modes are clear manifestations of this interaction.

The topological analysis clearly identify two different intermolecular N–H···S=C hydrogen bonds forming pseudo eight-membered rings between adjacent molecules. The NBO analysis allowed to characterize the hyperconjugative lpS → σ^*(N–H) remote interaction as important factor of covalency for these bonds, respectively.

Acknowledgments

ACF and MFE are members of the Carrera del Investigador of CONICET (República Argentina). The Argentine authors thank the Consejo Nacional de Investigaciones Científicas y Técnicas (CONICET), the ANPCYT and the Facultad de Ciencias Exactas, Universidad Nacional de La Plata for financial support.

Appendix A. Supplementary data

Supplementary data associated with this article can be found, in the online version, at http://dx.doi.org/10.1016/j.saa.2015.02.042.

References

[1] K.S. Eccles, R.E. Morrison, A.R. Maguire, S.E. Lawrence, Cryst. Growth Des. 14 (2014) 2753.
[2] E. Neucki, Ber. Dtsch. Chem. Ges. 6 (1873) 598.
[3] K.R. Koch, Coord. Chem. Rev. 216–217 (2001) 473.
[4] A.A. Aly, E.K. Ahmed, K.M. El-Mokadem, M.E.-A.F. Hegazy, J. Sulfur Chem. 28 (2007) 73.
[5] A. Saeed, U. Flörke, M.F. Erben, J. Sulfur Chem. 35 (2014) 318.
[6] Y.Y. Kharitonov, T.N. Gushchina, A.V. Gusev, N.I. Kirillova, Zh. Neorg. Khim. 33 (1988) 2228.
[7] S. Aruna, G. Shanmugam, S. Manogaran, D.N. Sathyanarayana, Bull. Chem. Soc. Jpn. 55 (1982) 3612.
[8] M.G. Woldu, J. Dillen, Theor. Chem. Acc. 121 (2008) 71.
[9] A.M. Plutín, H. Márquez, E. Ochoa, M. Morales, M. Sosa, L. Morán, Y. Rodríguez, M. Suárez, N. Martín, C. Seoane, Tetrahedron 56 (2000) 1533.
[10] A. Okuniewski, J. Chojnacki, B. Becker, Acta Crystallogr. E68 (2012) o619.
[11] A. Saeed, U. Flörke, Acta Crystallogr. E63 (2007) o3695.
[12] O. Estévez-Hernández, E. Otazo-Sánchez, J.L. Hidalgo-Hidalgo de Cisneros, I. Naranjo-Rodríguez, E. Reguera, Spectrochim. Acta A62 (2005) 964.
[13] H. Perez, R.S. Correa, A.M. Plutin, A. Alvarez, Y. Mascarenhas, Acta Crystallogr. E 67 (2011) o647.
[14] H. Perez, R.S. Correa, A.M. Plutin, B. O'Reilly, M.B. Andrade, Acta Crystallogr. C 68 (2012) o19.
[15] M. Boiocchi, L. Del Boca, D.E. Gomez, L. Fabbrizzi, M. Licchelli, E. Monzani, J. Am. Chem. Soc. 126 (2004) 16507.
[16] M. Bonizzoni, L. Fabbrizzi, A. Taglietti, F. Tiengo, Eur. J. Org. Chem. 2006 (2006) 3567.
[17] H.-L. Chen, Z.-F. Guo, Z.-L. Lu, Org. Lett. 14 (2012) 5070.
[18] S. Li, X. Cao, C. Chen, S. Ke, Spectrochim. Acta 96A (2012) 18.
[19] A. Solinas, H. Faure, H. Roudaut, E. Traiffort, A. Schoenfelder, A. Mann, F. Manetti, M. Taddei, M. Ruat, J. Med. Chem. 55 (2012) 1559.
[20] C. Limban, A.-V. Missir, I.C. Chirita, A.F. Neagu, C. Draghici, M.C. Chifiriuc, Rev. Chim. (Bucharest) 62 (2011) 168.
[21] C. Limban, A.-V. Missir, I.C. Chirita, C.D. Badiceanu, C. Draghici, M.C. Balostescu, O. Stamatoiu, Rev. Roum. Chim. 53 (2008) 595.
[22] J. Müller, C. Limban, B. Stadelmann, A.V. Missir, I.C. Chirita, M.C. Chifiriuc, G.M. Nitulescu, A. Hemphill, Parasitol. Int. 58 (2009) 128.
[23] J. Sun, S. Cai, H. Mei, J. Li, N. Yan, Q. Wang, Z. Lin, D. Huo, Chem. Biol. Drug Des. 76 (2010) 245.
[24] X. Su, G. Zhang, T. Liu, L. Chen, J. Qin, C. Chen, Inorg. Chem. Commun. 9 (2006) 986.
[25] A. Saeed, M.F. Erben, U. Shaheen, U. Flörke, J. Mol. Struct. 1000 (2011) 49.
[26] A. Saeed, M.F. Erben, M. Bolte, J. Mol. Struct. 985 (2010) 57.
[27] M. Khawar Rauf, A. Badshah, M. Bolte, Acta Crystallogr. E 62 (2006) o4084.
[28] A. Saeed, M.F. Erben, U. Flörke, J. Mol. Struct. 982 (2010) 91.
[29] M. Khawar Rauf, A. Badshah, A. Saeed, M. Bolte, Acta Crystallogr. E 62 (2006) o1262.
[30] H. Arslan, N. Külcü, U. Flörke, Spectrochim. Acta 64A (2006) 1065.
[31] H. Arslan, U. Flörke, N. Külcü, G. Binzet, Spectrochim. Acta 68A (2007) 1347.
[32] A.E. Reed, R.B. Weinstock, F. Weinhold, J. Chem. Phys. 83 (1985) 735.
[33] J.P. Foster, F. Weinhold, J. Am. Chem. Soc. 102 (1980) 7211.
[34] R.F.W. Bader, J.R. Cheeseman, K.E. Laidig, K.B. Wiberg, C. Brenemad, J. Am. Chem. Soc. 112 (1990) 6530.
[35] I.B. Douglass, F.B. Dains, J. Am. Chem. Soc. 56 (1934) 719.
[36] M.J. Frisch, G.W. Trucks, H.B. Schlegel, G.E. Scuseria, M.A. Robb, J.R. Cheeseman, J.A. Montgomery Jr., T. Vreven, K.N. Kudin, J.C. Burant, J.M. Millam, S.S. Iyengar, J. Tomasi, V. Barone, B. Mennucci, M. Cossi, G. Scalmani, N. Rega, G.A. Petersson, H. Nakatsuji, M. Hada, M. Ehara, K. Toyota, R. Fukuda, J. Hasegawa, M. Ishida, T. Nakajima, Y. Honda, O. Kitao, H. Nakai, M. Klene, X. Li, J.E. Knox, H.P. Hratchian, J.B. Cross, C. Adamo, J. Jaramillo, R. Gomperts, R.E. Stratmann, O. Yazyev, A.J. Austin, R. Cammi, C. Pomelli, J.W. Ochterski, P.Y. Ayala, K. Morokuma, G.A. Voth, P. Salvador, J.J. Dannenberg, V.G. Zakrzewski, S. Dapprich, A.D. Daniels, M.C. Strain, O. Farkas, D.K. Malick, A.D. Rabuck, K. Raghavachari, J.B. Foresman, J.V. Ortiz, Q. Cui, A.G. Baboul, S. Clifford, J. Cioslowski, B.B. Stefanov, G. Liu, A. Liashenko, P. Piskorz, I. Komaromi, R.L. Martin, D.J. Fox, T. Keith, M.A. Al-Laham, C.Y. Peng, A. Nanayakkara, M. Challacombe, P.M.W. Gill, B. Johnson, W. Chen, M.W. Wong, C. Gonzalez, J.A. Pople, Gaussian 03, Revision C.02, Gaussian Inc, Wallingford CT, 2004.
[37] M.J. Frisch, J.A. Pople, J.S. Binkley, J. Chem. Phys. 80 (1984) 3265.
[38] A. Fu, D. Du, Z. Zhou, Spectrochim. Acta 59A (2003) 245.
[39] R. Dovesi, R. Orlando, B. Civalleri, C. Roetti, V.R. Saunders, C.M. Zicovich-Wilson, Z. Kristallogr. 220 (2005) 571.
[40] R. Dovesi, V.R. Saunders, C. Roetti, R. Orlando, C.M. Zicovich-Wilson, F. Pascale, B. Civalleri, K. Doll, N.M. Harrison, I.J. Bush, P. D'Arco, M. Llunell, CRYSTAL09 User's Manual, University of Torino, Torino, 2009.
[41] C. Gatti, TOPOND 98 User's Manual, CNR-ISTM, Milano, 1999.
[42] A. Spek, J. Appl. Crystallogr. 36 (2003) 7.
[43] G. Sheldrick, Acta Crystallogr. A 64 (2008) 112.
[44] K. Gholivand, S. Farshadian, M.F. Erben, C.O. Della Védova, J. Mol. Struct. 978 (2010) 67.
[45] W. Yang, W. Zhou, Z. Zhang, J. Mol. Struct. 828 (2007) 46.
[46] F. Aydin, H. Ünver, D. Aykaç, N.O. Iskeleli, J. Chem. Crystallogr. 40 (2010) 1082.
[47] L. Adane, P.V. Bharatam, Int. J. Quantum Chem. 108 (2008) 1277.
[48] H. Arslan, D.S. Mansuroglu, D. VanDerveer, G. Binzet, Spectrochim. Acta 72A (2009) 561.
[49] S.A. Slivko, Y.Y. Kharitonov, S.L. Kuznetsov, T.N. Glushchina, J. Struct. Chem. 34 (1993) 225.
[50] Z. Weiqun, L. Kuisheng, Z. Yong, L. Lu, J. Mol. Struct. 657 (2003) 215.
[51] Z. Weiqun, L. Baolong, Z. Baolong, D. Jiangang, Z. Yong, L. Lude, Y. Xujie, J. Mol. Struct. 690 (2004) 145.
[52] M. Atiş, F. Karipcin, B. Sarıboğa, M. Taş, H. Çelik, Spectrochim. Acta 98A (2012) 290.
[53] O. Hritzová, J. Cernák, P. Safar, Z. Frohlichová, I. Csoregh, J. Mol. Struct. 743 (2005) 29.
[54] A. Saeed, M.F. Erben, M. Bolte, Spectrochim. Acta 102A (2013) 408.
[55] W. Zhu, W. Yang, W. Zhou, H. Liu, S. Wei, J. Fan, J. Mol. Struct. 1004 (2011) 74.
[56] F. Karipcin, M. Atis, B. Sariboga, H. Celik, M. Tas, J. Mol. Struct. 1048 (2013) 69.
[57] K.J. Rothschild, I.M. Asher, H.E. Stanley, E. Anastassakis, J. Am. Chem. Soc. 99 (1977) 2032.
[58] O. Estévez-Hernández, E. Otazo-Sánchez, J.L.H.-H.d. Cisneros, I. Naranjo-Rodríguez, E. Reguera, Spectrochim. Acta A64 (2006) 961.
[59] N. Selvakumaran, M.M. Sheeba, R. Karvembu, S.W. Ng, E.R.T. Tiekink, Acta Crystallogr. E 68 (2012) o3259.
[60] N. Gunasekaran, P. Jerome, R. Karvembu, S.W. Ng, E.R.T. Tiekink, Acta Crystallogr. E 67 (2011) o1149.
[61] B.M. Yamin, E.A. Othman, Acta Crystallogr. E 64 (2008) o313.
[62] I.N. Hassan, B.M. Yamin, M.B. Kassim, Acta Crystallogr. E 66 (2010) o2796.
[63] E. Espinosa, M. Souhassou, H. Lachekar, C. Lecomte, Acta Crystallogr. B 55 (1999) 563.
[64] J. Bernstein, M.C. Etter, L. Leiserowitz, The Role of Hydrogen Bonding in Molecular Assemblies, Wiley-VCH Verlag GmbH, 2008.
[65] A.G. Dikundwar, U.D. Pete, C.M. Zade, R.S. Bendre, T.N. Guru Row, Cryst. Growth Des. 12 (2012) 4530.
[66] L.R. Gomes, L.M.N.B.F. Santos, J.A.P. Coutinho, B. Schroder, J.N. Low, Acta Crystallogr. E 66 (2010) o870.
[67] U. Adhikari, S. Scheiner, J. Phys. Chem. A 116 (2012) 3487.
[68] A.J. Lopes Jesus, M.T.S. Rosado, I. Reva, R. Fausto, M.E.S. Eusébio, J.S. Redinha, J. Phys. Chem. A 112 (2008) 4669.
[69] A.E. Reed, L.A. Curtiss, F. Weinhold, Chem. Rev. 88 (1988) 899.
[70] A. Saeed, A. Khurshid, J.P. Jasinski, C.G. Pozzi, A.C. Fantoni, M.F. Erben, Chem. Phys. 431–432 (2014) 39.
[71] L. Aguilar-Castro, M. Tlahuextl, L.H. Mendoza-Huizar, A.R. Tapia-Benavides, H. Tlahuext, ARKIVOC (2008) 210.
[72] G.R. Desiraju, Acc. Chem. Res. 35 (2002) 565.